

Improved Method for Prediction of Noise from Single Jets

K. Viswanathan*

The Boeing Company, Seattle, Washington 98124-2207

DOI: 10.2514/1.23202

The prediction of jet noise from first principles has proved to be elusive. Practical methods rely on empirical correlations of experimental measurements, supplemented by some theoretical considerations and ad hoc functions. Clearly, these empirical methods are only as good as the databases on which they are based. An experimental aeroacoustic database of high quality created by the author and subsequent scaling laws derived using the database have facilitated the development of an accurate prediction method. The scaling laws, wherein the spectral shape at any radiation angle is expressed as a function of the jet velocity ratio and the jet stagnation temperature ratio, allow the spectra at different jet velocities but at a fixed jet stagnation temperature to be collapsed to a single curve at each radiation angle. Thus, master spectra as a function of the Strouhal number are developed. No additional empiricism or other factors are needed. The range of the Strouhal number has been extended considerably through the use of nozzles of different diameters and the acquisition of accurate data up to a one-third octave center band frequency of 80 KHz. The master spectra developed here can be used to predict the turbulent mixing noise as well as check the quality of the data.

Nomenclature

A	=	nozzle exit area, square inch
AA	=	atmospheric absorption coefficient, dB/ft
a	=	ambient speed of sound
D	=	nozzle exit diameter
$D(\phi)$	=	directivity factor
f	=	frequency, Hz
I	=	overall sound pressure level or noise intensity
M	=	jet Mach number
M_c	=	convective Mach number ($=0.7 \times V_j/a$)
n	=	velocity exponent
r	=	observer distance
St	=	Strouhal number (fD/V_j)
T_a	=	ambient temperature
T_t	=	jet stagnation temperature
V, V_j	=	jet velocity
α	=	constant in directivity factor
ϕ	=	exhaust angle, degree
θ	=	inlet angle, degree

I. Introduction

THE prediction of jet noise from first principles has proved to be elusive because of the complex nature of the turbulence in high-speed jets and the complex mechanisms of noise generation, which are not well understood. The acoustic analogy of Lighthill [1], and its subsequent variants and extensions by other researchers, have been used widely in the analysis of jet noise for the past 50 years. There were numerous theoretical and experimental investigations of jet noise in the 1970s and early 1980s; a brief list of these may be found in [2–11]. Many scaling laws and prediction methods based on the acoustic analogy have also been attempted; see Lilley [12] for a detailed review of these types of methodologies. In spite of all these efforts, no practical prediction method has emerged and there is no

consensus on a jet noise theory or on the nature of the acoustic sources in a high-speed jet. From a practical standpoint, accurate spectral predictions over a wide range of frequencies are required at all radiation angles. Given the above scenario vis-à-vis predictions based on the governing equations of motion, it has been necessary to formulate empirical prediction methods. These are based on empirical correlations of experimental data, with the incorporation of some scaling laws supplemented by many ad hoc functions and factors that provide good fit with data.

The recommended methods for various noise components have been compiled by the Society of Automotive Engineers (SAE) [13]. For a single stream jet, the noise prediction procedure for the static case is as follows. A carpet plot of the normalized free-field overall sound pressure levels has been compiled as functions of acoustic Mach number (V_j/a) and radiation angle. For given jet reservoir condition, the overall sound pressure level (OASPL) at a particular angle is determined by the appropriate summation of the expressions for the size (area) of the nozzle, observer distance, density correction and pressure normalization to the normalized OASPL obtained from the carpet plot. Master spectral shapes in terms of $[SPL(f) - OASPL]$ as a function of normalized Strouhal number have also been determined for each angle at different stagnation temperature ratios (T_t/T_a). From these master spectra, one can obtain the jet noise spectra at desired angles and observer distance. For flight noise prediction, a similar procedure is followed, with the OASPL adjusted to account for the relative velocity effect. This adjustment term is a function of $(V_j - V_a)$, where V_a is the flight velocity, raised to a relative velocity exponent, which is a function of angle and velocity ratio. The normalized Strouhal number also incorporates the term $(V_j - V_a)$ as the reference velocity. A comprehensive list of the major studies that provided the basis for this recommended methodology is given in [13]. Though this method provides reasonable predictions over a wide range of jet velocities and operating conditions, the accuracy of the predictions are not within the limits required for industry applications.

Given that the practical prediction methods rely on experimental databases, the accuracy of the predictions depends very much on the quality of these data. Viswanathan [14–17] addressed the many pitfalls associated with aeroacoustic testing and reported on the rig refurbishment efforts that led to improved spectral measurements. An examination of existing databases from five jet noise laboratories revealed that most of the data are contaminated. Consequently, existing empirical prediction methods based on these data are suspect.

Recently, Viswanathan [18] developed new scaling laws and demonstrated excellent spectral collapse over the entire frequency

Presented as Paper 2935 at the 11th AIAA/CEAS Aeroacoustics Conference, Monterey, CA, 23–25 May 2005; received 14 February 2006; revision received 14 May 2006; accepted for publication 7 June 2006. Copyright © 2006 by The Boeing Company. Published by the American Institute of Aeronautics and Astronautics, Inc., with permission. Copies of this paper may be made for personal or internal use, on condition that the copier pay the \$10.00 per-copy fee to the Copyright Clearance Center, Inc., 222 Rosewood Drive, Danvers, MA 01923; include the code \$10.00 in correspondence with the CCC.

*Associate Technical Fellow, Aeroacoustics and Fluid Mechanics, MS 67-ML, P.O. Box 3707; k.viswanathan@boeing.com. Associate Fellow AIAA.

range. Two practical applications, an accurate prediction method and a quantitative means for checking the data quality, are natural by-products of the scaling methodology. This paper is organized as follows: a brief description of the databases is first provided, followed by a short overview of the scaling laws and the prediction method. Additional issues that need to be addressed for scaling spectra at angles close to the jet axis are then discussed.

II. Experimental Database

A comprehensive aeroacoustic database, from unheated and heated jets over a wide range of Mach numbers and stagnation temperature ratios, has been developed. Detailed descriptions of the test facility, the jet simulator, the data acquisition and reduction process, etc., may be found in Viswanathan [14]. Salient results from this database have already been published in [14–18]. For the sake of completeness, a brief overview is provided here. The jet simulator is embedded in an open-jet wind tunnel, which can provide a maximum freestream Mach number of 0.32. The takeoff Mach numbers for all commercial aircraft fall in the range of 0.24 to 0.30; hence, the effects of forward flight can be evaluated at realistic freestream velocities in Boeing's Low Speed Aeroacoustic Facility. Bruel and Kjaer quarter-inch Type 4939 microphones are used for free-field measurements. The microphones are set at normal incidence and without the protective grid, which yields a flat frequency response up to 100 KHz. Typically, several linear microphone arrays are used. The microphones in each array are laid out at a constant sideline distance of 15 ft (4.572 m) from the jet axis. Very fine narrow band data with a bin spacing of 23.4 Hz up to a maximum frequency of 88,320 Hz are acquired and synthesized to produce one-third octave spectra, with a center band frequency range of 200 to 80,000 Hz.

Figure 1 shows the test matrix, in which the stagnation temperature ratio (T_t/T_a) was held constant at values of 1.0, 1.8, 2.2, 2.7, and 3.2. Throughout this paper, the stagnation or total temperature ratio is quoted. Unless otherwise stated, the terminology "jet temperature ratio" denotes the stagnation temperature ratio. At each jet temperature, the nozzle pressure ratio (NPR) was varied systematically so as to produce jets at Mach numbers (M) of 0.3, 0.4, 0.5, 0.6, 0.7, 0.8, 0.9, 1.0, 1.24, 1.36, 1.47 and 1.58. Figure 2 shows the range of the jet velocity (V_j/a) for the various temperature ratios; attention is drawn to the fact that there is considerable overlap. As denoted by the thick dashed vertical line, the velocity for the unheated jet at $M = 1.0$ is greater than those for the lowest five Mach numbers for heated jets with $T_t/T_a = 1.8$, etc. Apart from this main test matrix, data were taken at other jet conditions as well. It was

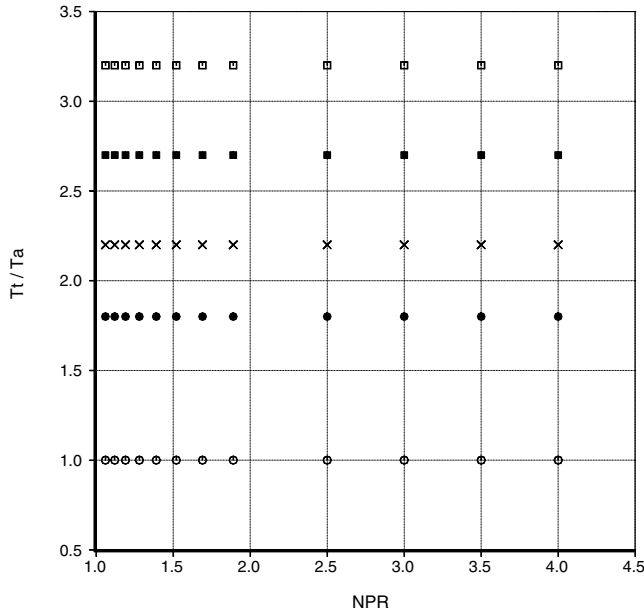


Fig. 1 The main test matrix.

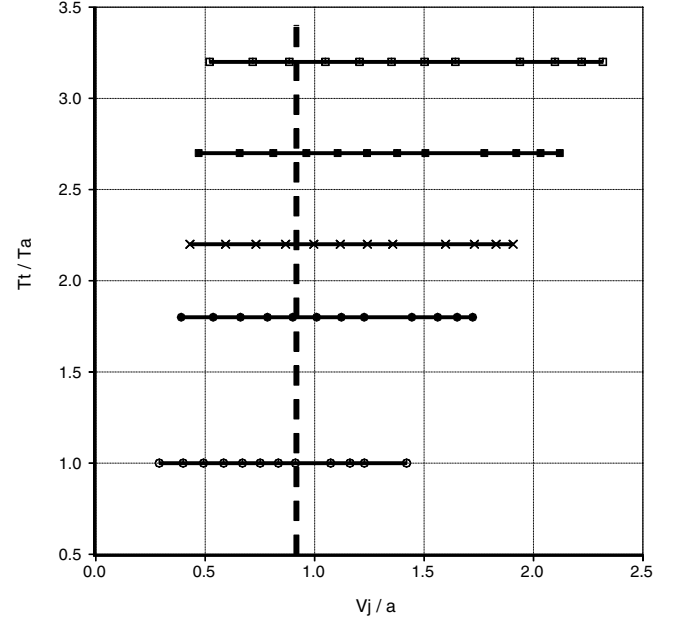


Fig. 2 Variations of the acoustic Mach number (V_j/a) for different jet temperature ratios. \circ : $T_t/T_a = 1.0$; \bullet : $T_t/T_a = 1.8$; \times : $T_t/T_a = 2.2$; \blacksquare : $T_t/T_a = 2.7$; \square : $T_t/T_a = 3.2$.

demonstrated clearly in [14–18] that the noise data are of the highest quality over the entire frequency range. Nozzles of different diameters have also been used to acquire data at the above jet conditions. The use of larger nozzles and accurate measurements up to 80 KHz, have extended the Strouhal number range considerably in the current database.

III. Overview of the Scaling Laws

The scaling laws are based on the observations that 1) the overall sound power level (OAPWL) has a weak dependence on the jet temperature ratio, and 2) the OASPL at any angle depends on the temperature ratio. Therefore, the scaling laws for the OAPWL, and the OASPL at any angle (θ), may be written as

$$\text{sound power} \propto \left(\frac{V_j}{a}\right)^n, \quad n = n\left(\frac{T_t}{T_a}\right)$$

$$I_\theta \propto \left(\frac{V_j}{a}\right)^n, \quad n = n\left(\theta, \frac{T_t}{T_a}\right)$$

The velocity exponent for both the OAPWL and the OASPL depend on the temperature ratio; see [15,18] for additional details. Viswanathan [18] demonstrated excellent spectral collapse at the lower radiation angles over the entire frequency range with these simple scaling laws and showed unambiguously that the proposed formulation allows for the mixing noise spectra to be represented by

$$\text{SPL}(\theta, St) = f\left(\frac{T_t}{T_a}, n\right), \quad n = n\left(\theta, \frac{T_t}{T_a}\right)$$

This is the main outcome of the scaling laws that permits the development of the prediction methodology. No other assumptions or multiplicative functions that depend on the Strouhal number are needed, as clear-cut spectral shapes at any angle are determined by the two independent parameters of the velocity ratio (V_j/a) and the temperature ratio (T_t/T_a).

IV. Prediction Method for Turbulent Mixing Noise

It is immediately obvious that the scaling methodology can be used to generate normalized or master spectra, which would form the basis for an empirical prediction method for turbulent mixing noise as well as provide accurate spectra for the development and

assessment of prediction methods. The main test matrix here covers a Mach number range of 0.3 to 1.0 and a temperature ratio range of 1.0 to 3.2. The measured spectra are normalized to a common polar distance of 20 ft from the center of the nozzle exit (coordinate system with origin at the center of the nozzle exit) and are converted to either lossless form or standard day conditions [ambient temperature of 77°F (298°K) and relative humidity of 70%] using the method of Shields and Bass [19]. The effect of the nozzle area (A) is removed in the normalization process, and the normalized spectral level per unit area may be written as

$$\text{SPL}_{(20 \text{ ft})} = \text{SPL}_{\text{measured}} - 10\log_{10}(A) - 10\log_{10}\left(\frac{20}{r}\right)^2 + r[AA_{(\text{test day})}] - 20[AA_{(\text{std day})}]$$

The above equation provides spectra corrected to standard day conditions; for lossless data, the last term on the right hand side of this equation is omitted. The usual practice of converting the as-measured data to lossless form and then propagating the spectra to a common distance (of 20 ft) while accounting for the atmospheric absorption at standard day conditions has been adopted. Implicit in this process is the assumption of linear propagation, with the sound pressure level obeying the $(1/r^2)$ dependence. The issue with propagation is examined in detail below. The accuracy of the weather corrections and the suitability of the different proposed methods have been evaluated by Viswanathan [17]; it was shown that the method of Shields and Bass [19] was the best at the higher frequencies of interest in model scale tests.

For any given jet temperature ratio, it is straightforward to calculate the velocity exponent that collapses the spectra, as a function of Strouhal number, at the various NPR or jet Mach numbers. This procedure can be carried out at every measurement angle, which covers a polar range of 50 to 155 deg or 160 deg in the data presented here. Therefore, one can generate master spectra, similar to the samples shown in [18] at all the angles and at all the temperature ratios, with the velocity exponent at each condition (angle and T_t/T_a) controlling the effect of the jet velocity (V_j/a) on the radiated noise levels. Additional evidence that this scaling approach indeed leads to master spectra is provided in Figs. 3 and 4. The parameter $[\text{SPL} - 10 \times \log_{10}(A) - 10 \times n \times \log_{10}(V_j/a)]$ is plotted on the y axis as a function of the Strouhal number. In the above relation, A is dimensional; one could express this area in terms of square inches, square feet, or square meters. Depending on the

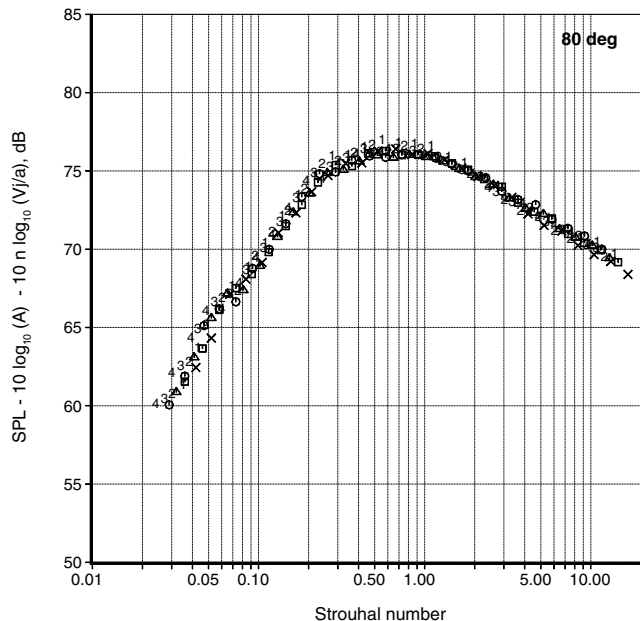


Fig. 3 Normalized spectra from heated jets at various Mach numbers. Symbols: $T_t/T_a = 2.2$; numbers: $T_t/T_a = 3.2$.

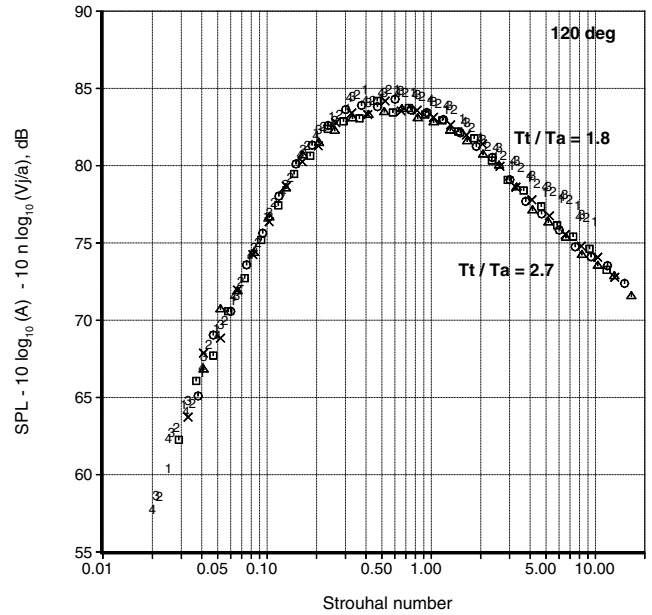


Fig. 4 Normalized spectra from heated jets at various Mach numbers.

chosen dimensional unit, the value of the spectral levels would move up or down by a scaling constant. For example, the noise per square foot would be higher than the noise per square inch by 21.58 dB $[10 \times \log_{10}(144)]$. However, a consistent use of the same dimensional unit should result in the correct noise levels, regardless of the unit chosen. The dimensional area in square inches is used here. Figure 3 shows that the normalized spectra at 80 deg from jets of different (V_j/a) at a fixed jet temperature ratio indeed collapse on to a single curve. Further, the spectral shapes at both temperature ratios of 2.2 and 3.2 are identical. Figure 4 shows another example at 120 deg at two different jet temperature ratios of 1.8 and 2.7. Again, there is excellent collapse over the entire Strouhal number range (measured frequency range of 200 Hz to 80 KHz).

Thus, the entire behavior of the turbulent mixing noise can be characterized by the three independent variables: the velocity exponent or (V_j/a), (T_t/T_a), and the radiation angle. This exercise has been carried out with the comprehensive database, with the analyses of the spectra at all the angles, Mach numbers, temperature ratios, and different nozzle diameters. Master spectra as a function of Strouhal number and the velocity exponents have been established from this exhaustive study and are reported now. The variation of the velocity exponent, as a function of angle and temperature ratio, already presented in Viswanathan [18], is reproduced here in Fig. 5 for the sake of completeness. At the lower polar angles, there is a substantial drop in the value of the exponent as the jet temperature ratio is progressively increased, from ~ 8.0 for the unheated case to ~ 5.2 for the highest T_t/T_a of 3.2. Further, the curves are quite flat in the forward quadrant for all T_t/T_a . As we move to the aft angles, the values start to increase, with the highest value of ~ 9.8 reached for the unheated jet at 155 deg. At an angle of 130 deg, we notice that all the heated jets have the same value for the velocity exponent. At further aft angles, the effect of jet temperature is seen to be minor, with the values of the velocity exponents more or less the same for all the temperature ratios, heated and unheated. That is, in the peak radiation sector, the effect of jet temperature on the velocity exponent is weak and the radiated noise depends only on (V_j/a). The normalized spectra above and most of the examples in [18] have been restricted to an angular region of 50 to 125 deg; a deeper analysis is needed in the peak radiation sector, as discussed below.

A. Unheated Jets

First, we address some additional issues that pertain to the spectra at large aft angles. There have been several attempts in the past ~ 30 years to develop normalized spectra, using different approaches. A popular one is the use of the acoustic analogy,

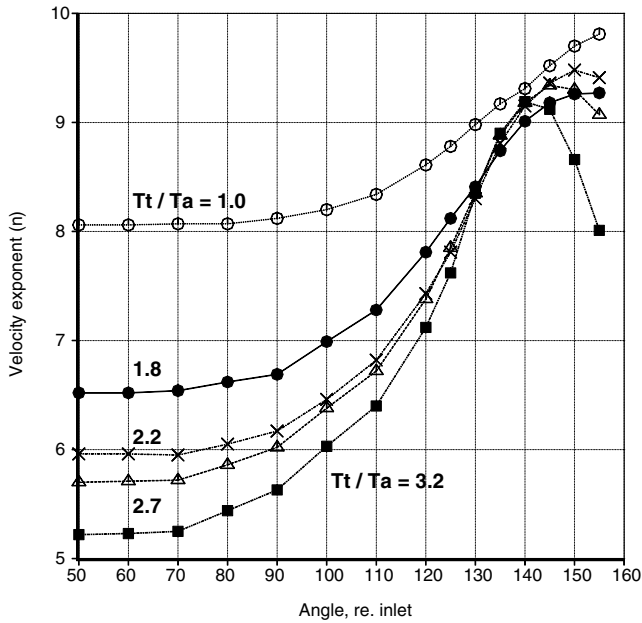


Fig. 5 Velocity exponent for various angles and temperature ratios.

combined with the concept of convective amplification for spectra in the aft angles. However, none of these efforts has yielded a satisfactory collapse of the data or an accurate prediction formula, even at 90 deg where the effects of convective amplification

$$D(\phi) = [(1 - M_c \cos \phi)^2 + \alpha^2 M_c^2]^{-5/2}$$

and the Doppler correction of frequency $[(fD/V_j) \times (1 - M_c \cos \phi)]$ are zero. ϕ is measured from the jet exhaust axis and M_c is the convective Mach number, usually assumed to be $\sim 0.7 \times (V_j/a)$ and α is an empirical constant with a value of ~ 0.3 . Other values of the power for the directivity factor from -3 to -9 (instead of -5), M_c , α , and various combinations thereof, have also been attempted but without much success. Some of the shortcomings associated with these approaches are investigated. Viswanathan [17] examined the consequence of using the Doppler correction for frequency in scaling spectra at the aft angles; see Sec. III.E in [17]. Two firm conclusions from the analysis are: 1) the inclusion of the Doppler factor destroys the excellent spectral collapse obtained without this factor, and 2) there is no experimental evidence for the concept of convective amplification. Therefore, this term is not used for scaling frequency.

The effect of applying the eighth-power law to spectra from unheated jets at two aft angles of 150 and 160 deg is shown in Figs. 6 and 7. There is good collapse of the spectra above a Strouhal number of ~ 0.5 ; however, there is no collapse at the spectral peak and at the lower frequencies. These types of figures can be seen in past studies, see Ahuja and Bushell [5], for example. The inclusion of correction terms for convective amplification, modified velocity, modified Strouhal number, etc., fail to collapse the spectra, as noted by Lush [2] and Ahuja and Bushell [5]. Hoch et al. [3], Tanna et al. [8], and Morfey et al. [11] noticed these trends and proposed two different ways of dealing with the observed trends: the introduction of a density exponent that is a function of (V_j/a) and the introduction of additional terms to include the effect of temperature fluctuations, which was assumed to follow the fourth or sixth power of (V_j/a) . Certain theoretical bases and a set of assumptions were invoked in the derivation of these scaling laws. As already mentioned, none of these approaches provided clear-cut scaling laws even for the OASPL. The fundamental difficulty lies in trying to develop scaling laws that are applicable to both unheated and heated jets, with the implicit assumption of a dominant V^8 effect somewhat modified by additional V^4 or V^6 dependence to account for the presumed changes in source strength and other effects mentioned in the above references. All these studies failed to note the weak dependence of

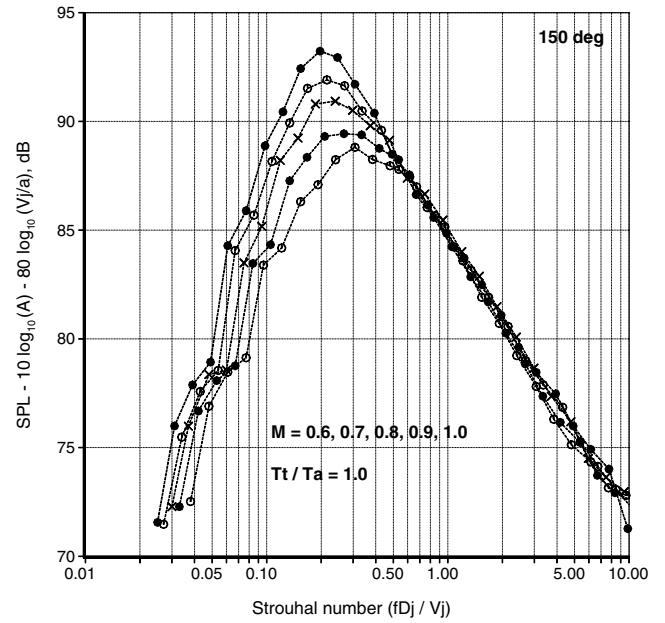


Fig. 6 Normalized spectra from unheated jets. Velocity exponent $n = 8$.

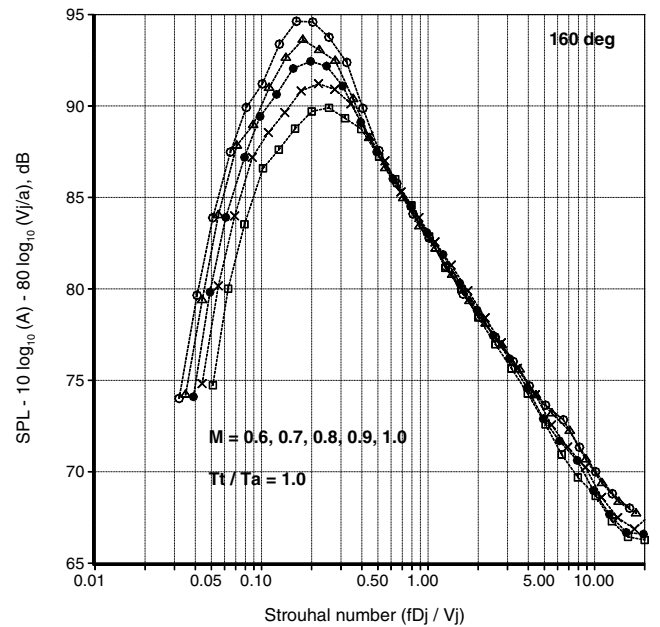


Fig. 7 Normalized spectra from unheated jets. Velocity exponent $n = 8$.

OAPWL on the temperature ratio and a stronger dependence of OASPL on the temperature ratio (especially at the lower angles), first observed by Viswanathan. Now we demonstrate how we can collapse the spectra shown in Fig. 7. Figure 8 shows the same data normalized with a velocity exponent of 9.8, instead of 8.0 as in Fig. 7. It is obvious that there is better collapse at the spectral peak and at the lower frequencies but a larger scatter at the higher Strouhal numbers to the right of the spectral peak. The reason for this is simple: at these aft angles, the peak frequency is independent of jet velocity, see Fig. 19 in [15]. Therefore, the wrong characteristic velocity scale is used for the normalized frequency on the x axis. If we now use the Helmholtz number $[fD/a]$ instead of the Strouhal number and replot the data in Fig. 9, we notice that the data collapse is excellent at the two large aft angles of 155 and 160 deg. Notice the drastic difference in the scaled spectra shown in Figs. 7 and 9. This example illustrates clearly that the correct choice of the independent variable is essential in developing the scaling relations for spectra at the aft angles.

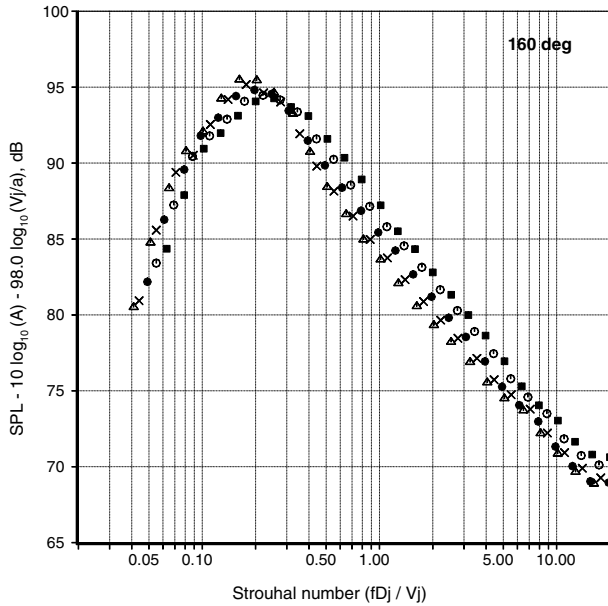


Fig. 8 Normalized spectra from unheated jets as a function of Strouhal number. $T_i/T_a = 1.0$. Velocity exponent $n = 9.8$.

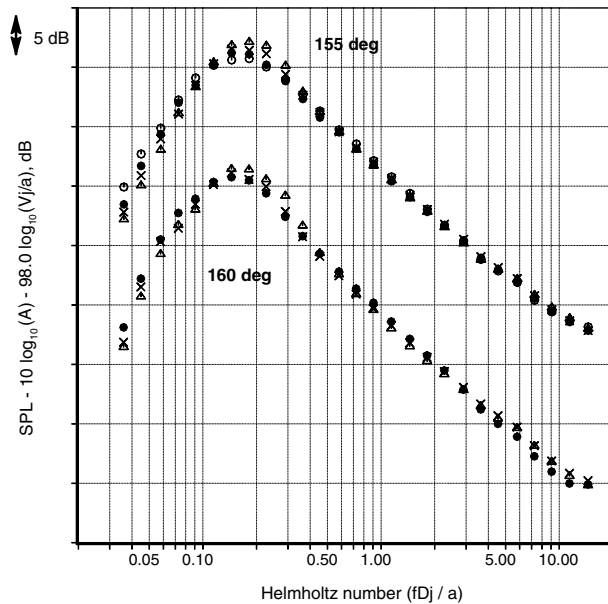


Fig. 9 Normalized spectra from unheated jets as a function of Helmholtz number. $T_i/T_a = 1.0$. Velocity exponent $n = 9.8$.

Whereas it is quite easy to determine the velocity exponent for OASPL, the spectral collapse requires a more careful analysis. It is obvious that the unmodified eighth-power law does not provide the proper scaling relations. Therefore, a clear recognition that the velocity exponent is a function of angle and temperature ratio and could be different from eight is essential in scaling jet noise spectra.

B. Heated Jets

The above example also highlights other potential complexities associated with the scaling of spectra at large aft angles for heated jets. Figure 10 shows spectra at an angle of 160 deg from jets at various Mach numbers and at a temperature ratio of 3.2. It is obvious that the spectral shapes are vastly different between the lower Mach number jets of 0.7 and 0.8 and the higher Mach numbers. Given the vast disparity in the jet velocities, from 1360 ft/s (415 m/s) for the $M = 0.7$ jet to 2607 ft/s (795 m/s) for the $M = 1.58$ jet, it is not surprising that the spectral peak is at a low Strouhal number for the

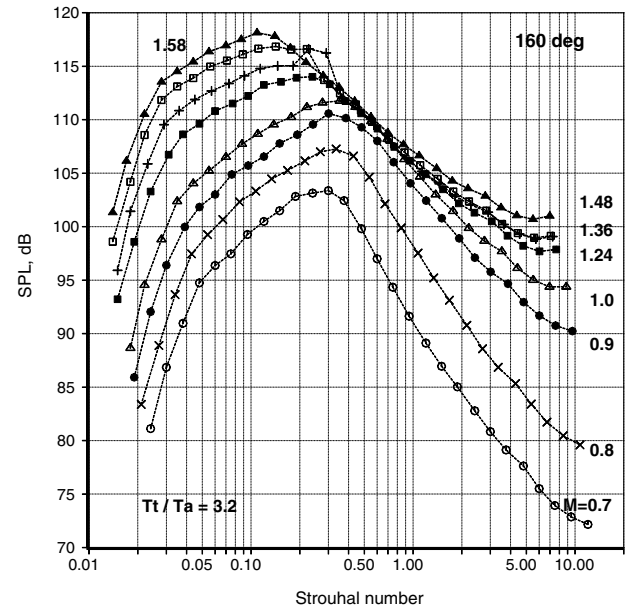


Fig. 10 Spectra from heated jets as a function of Strouhal number. $T_i/T_a = 3.2$.

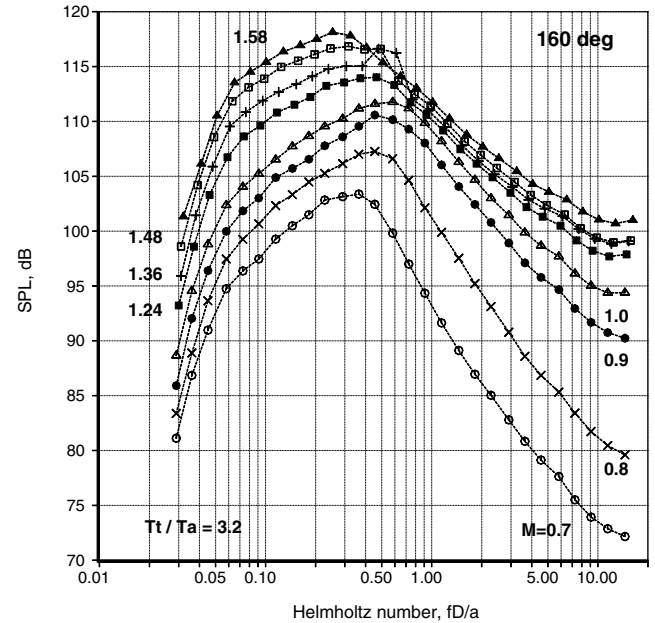


Fig. 11 Spectra from heated jets as a function of Helmholtz number.

$M = 1.58$ jet. For the supersonic Mach numbers, the fully expanded jet diameter is used instead of the geometric or physical diameter of the nozzle. The fully expanded jet diameter for both convergent and CD nozzles for any jet Mach number can be calculated using the formula developed by Tam and Tanna [20]. The same data are plotted as a function of Helmholtz number in Fig. 11. Though there is better alignment of the spectral peaks for the various Mach numbers, a single peak frequency that corresponds to all the cases can not be identified. This is so even for the subsonic heated jets in both Figs. 10 and 11; contrast this trend with that seen at a lower angle of 80 deg shown in Fig. 3. Viswanathan [15] observed that the peak frequency in these directions is independent of jet velocity as long as the acoustic Mach number is less than unity; at supersonic values of (V_j/a) , the peak values shift to higher frequencies. Further, there is a tremendous broadening of the spectral peak at the higher Mach numbers and a significant increase in levels at the lower frequencies; see Figs. 20–22 and associated discussion in [15].

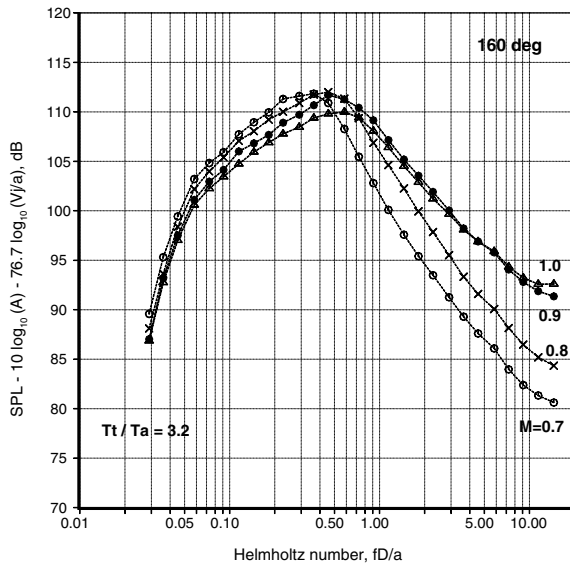


Fig. 12 Normalized spectra from heated jets as a function of Helmholtz number. $n = 7.67$. Subsonic jets.

An attempt to collapse the spectra at the subsonic Mach numbers as a function of Helmholtz number is shown in Fig. 12. The appropriate velocity exponent of 7.67 is used. At Mach numbers of 0.7 ($V_j/a = 1.2$) and 0.8 ($V_j/a = 1.35$), there is a mismatch between the spectral peaks. At the higher Mach numbers of 0.9 and 1.0, this mismatch is more pronounced, reflecting the trend noted in [15]. There is a more glaring difference at the higher frequencies, with the levels being ~ 7 dB higher for the $M = 0.9$ and $M = 1.0$ jets. It so happens that the convective Mach number, defined as the ratio of the convective velocity to the ambient speed of sound, becomes supersonic for these two jet Mach numbers. [The average convective velocity is taken to be $\approx 70\%$ of the jet velocity, which has been established in many experiments]. Viswanathan [17] demonstrated that nonlinear propagation effects manifest themselves when the convective Mach number exceeds unity, see Fig. 11 in this reference. Figure 10 in [17] indicates that the spectral level at the very high frequencies could be higher by ~ 7 dB for the $M = 0.9$ jet with $T_t/T_a = 3.2$, if the measurement distance is 30 ft (nondimensional distance, $r/D = 150$) instead of 10 ft ($r/D = 52$). Measurements at both of these distances are in the true far-field of jet noise, as shown in [16]. However, there is a big difference in the measured spectral levels at the higher frequencies when the measurement distance is very large for jets with supersonic convective Mach numbers. This phenomenon has not been noted earlier. It is worth noting that if the spectra at the closer microphone ($r/D = 52$) are used, much of the discrepancy noted in Fig. 12 at the higher frequencies would disappear. Thus, the nonlinear propagation effects further complicate an already tenuous situation in scaling spectra from highly heated jets in the peak radiation angles. However, it is quite straightforward to scale the OASPL for this particular temperature ratio, as shown in Fig. 33 in Viswanathan [15].

Figure 13 shows the normalized spectra for the two high subsonic Mach numbers and two supersonic Mach numbers of 1.24 and 1.58. Although there is reasonable agreement between the two subsonic spectra (not quite as good as at the lower polar angles, see Figs. 3 and 4), the mismatch increases with Mach number (or V_j/a). A reexamination of Fig. 11 indicates that there is negligible rise in spectral levels at the higher frequencies (to the right of the spectral peak) with increasing jet Mach number. The variation of the directivity of OASPL at this temperature ratio for a wide range of jet Mach numbers is examined in Fig. 14. At the low subsonic Mach numbers, up to $M = 0.9$, the peak radiation occurs at ~ 150 deg. With a further increase in Mach number at this fixed (T_t/T_a), the peak radiation shifts to lower angles, with virtually no increase in levels above a Mach number of 1.38 for emission angles greater than 135 deg. In this angular range, from 135 to 160 deg where turbulent

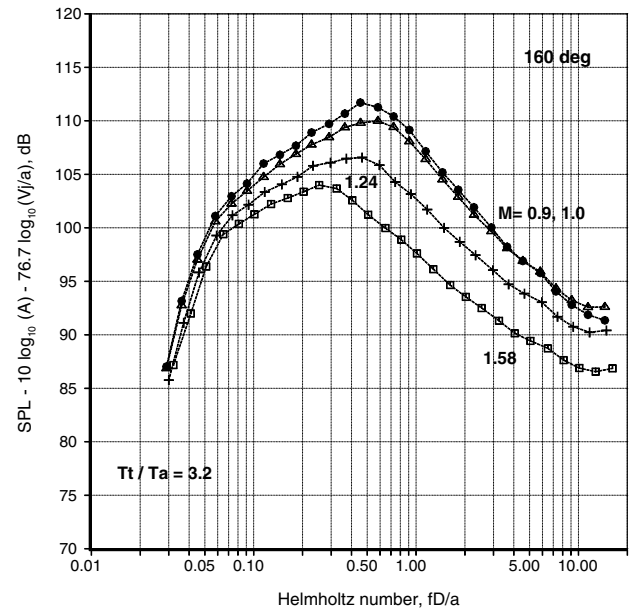


Fig. 13 Normalized spectra from heated jets as a function of Helmholtz number. $n = 7.67$. Subsonic and supersonic jets.

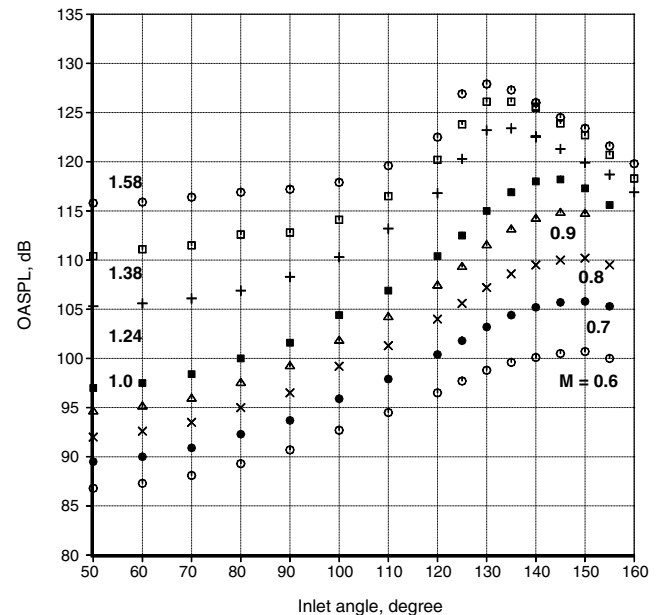


Fig. 14 Polar directivity of OASPL of heated jets at various jet Mach numbers. $T_t/T_a = 3.2$.

mixing noise is the dominant component (except for screech tones and possible amplification of mixing noise by these tones as described by Viswanathan [18]), the scaling law evidently does not follow the trends seen for subsonic Mach numbers. Therefore, the scaling laws based on subsonic Mach numbers will not be applicable for the supersonic Mach numbers in the peak radiation angles. This is the reason for the observed trend in Fig. 13.

C. Scaling Laws for Spectra in Peak Radiation Sector

The heated jet case presented above illustrates the complex issues that must be addressed in scaling spectra. The angle of 160 deg was selected to highlight the different issues; it must be clearly recognized, though, that the entire peak radiation sector requires special treatment. We now establish the angular range where the above effects need to be considered. Detailed spectral analyses of the entire database, at various angles and jet conditions, have been

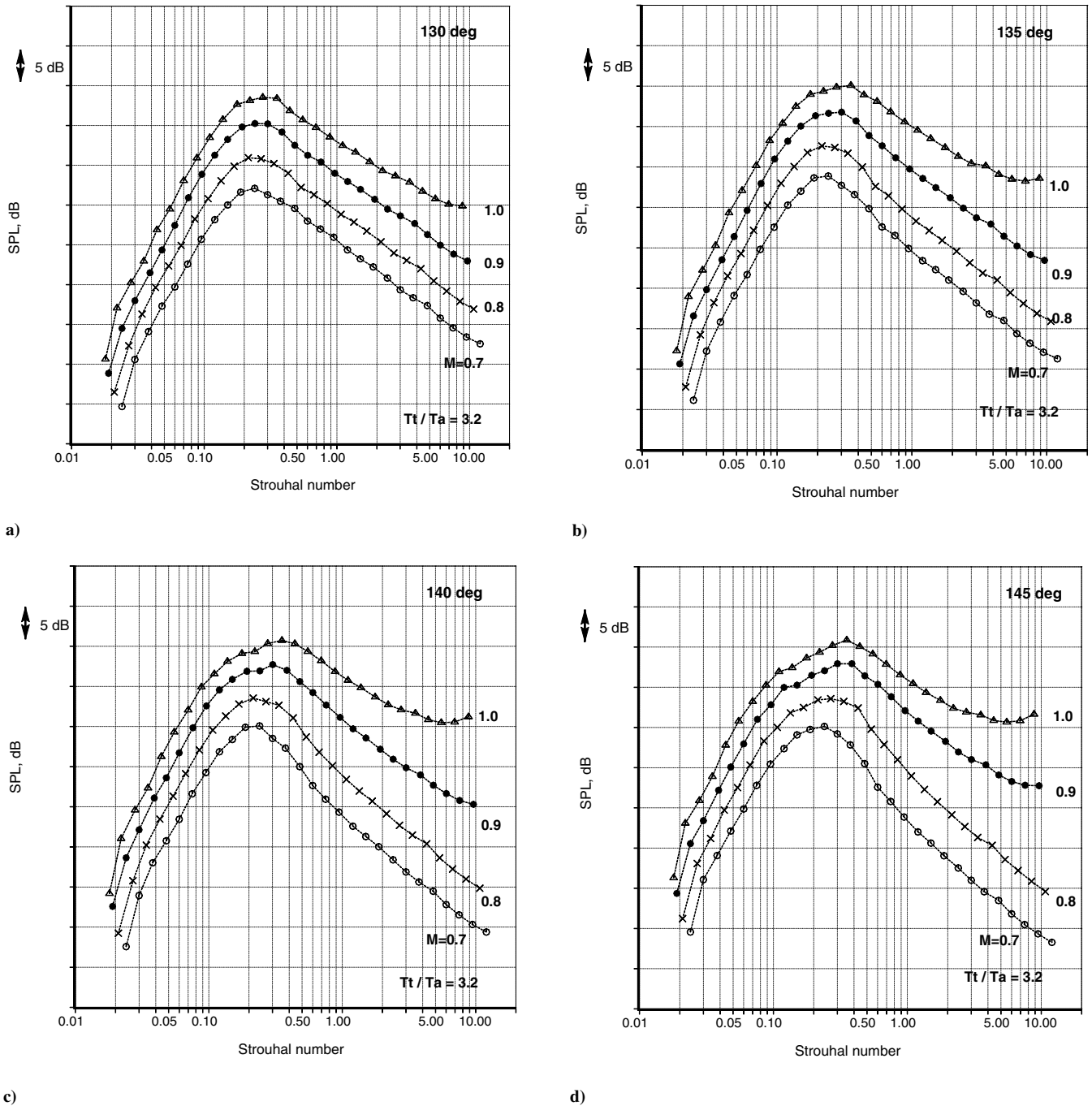


Fig. 15 Spectra from heated jets at different Mach numbers at several angles.

carried out. Figures 15a–15d show lossless spectra from jets at several Mach numbers and with $T_t/T_a = 3.2$, at angles of 130, 135, 140, and 145 deg, respectively. Although the spectral shapes at the lower two Mach numbers of 0.7 and 0.8 exhibit the same shape at all the angles, the spectra at the higher two Mach numbers of 0.9 and 1.0 do not. Recall that for these two higher jet Mach numbers, the convective Mach numbers are supersonic. At an angle of 130 deg, the nonlinear propagation effects as evidenced from the spectral slope (roll off) at the higher frequencies to the right of the peak are negligible. At an angle of 135 deg, the spectrum for the $M = 1.0$ jet starts curling up at the higher frequencies. As we move further aft, this trend becomes more pronounced for the $M = 1.0$ jet. At radiation angles of 145 deg and higher, the effects are clearly obvious for both the higher Mach numbers. Figures 16a and 16b show similar spectral comparisons at a lower temperature ratio of 2.7. At 130 deg, all the spectra have similar slopes to the right of the spectral peak, at least visually. At 145 deg, the spectrum from the $M = 1.0$ jet

exhibits nonlinear propagation effects. For the $M = 0.9$ jet at this lower temperature ratio, the convective Mach number is subsonic and no nonlinear propagation effect is discerned. These two sets of plots provide further confirmation of the role of the convective Mach number in triggering nonlinear propagation for jet noise; see Viswanathan [17] for additional information.

From the above sample results and additional analyses, it is concluded that the nonlinear effects are confined to a radiation sector of 130 deg and higher angles, at least up to a jet velocity of 1850 ft/s (564 m/s) for the $M = 1.0$ jet with $T_t/T_a = 3.2$. Quantitative confirmation is provided in Figs. 17a–17c, where the spectra have been collapsed at three angles of 120, 125, and 130 deg for five different jet Mach numbers of 0.6, 0.7, 0.8, 0.9, and 1.0 for these heated jets with $T_t/T_a = 3.2$. At 120 and 125 deg, we observe excellent collapse of the spectra for all the Mach numbers over the entire frequency range; the velocity exponents have been determined to be 7.46 and 7.98, respectively. At 130 deg, again there is excellent

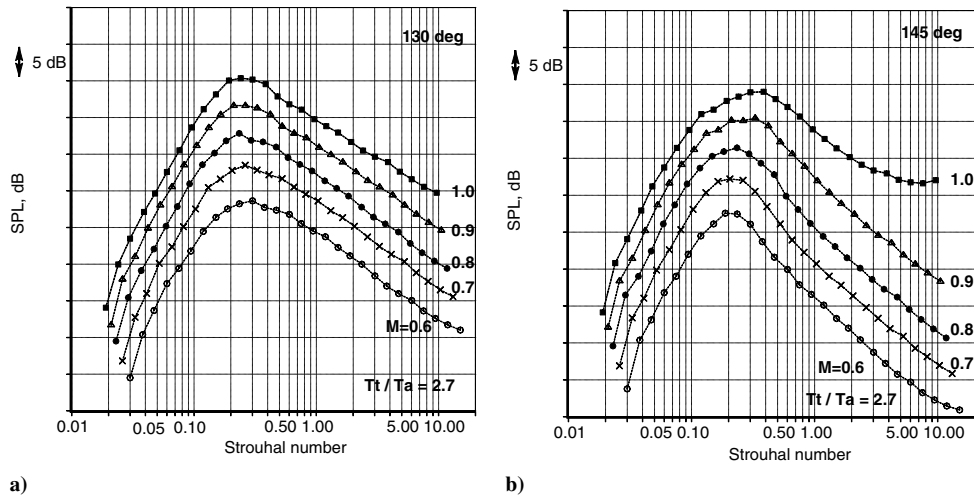


Fig. 16 Spectra from heated jets at different Mach numbers at several angles.

collapse for the lower 3 M numbers at all frequencies. For the jets at $M = 0.9$ and 1.0 , there is a slight increase in the levels at the highest frequencies. Currently, there is no analytical or numerical method available for the calculation of the nonlinear propagation effects over a given distance, with a specified pressure-time signal (or spectra) at an initial point in space. The highest temperature jets have been chosen purposely for this exercise; it should be obvious that at lower (V_j/a) , nonlinear effects are not a concern. Attention is also drawn to another feature in all these plots: the choice of the Strouhal number

without the Doppler correction provides the observed collapse. Therefore, it is safe to state that the spectra in the radiation sector that covers the forward quadrant and all the angles up to 130° can be collapsed with the appropriate velocity exponent as a function of jet temperature ratio and Strouhal number.

It has been established unambiguously that the scaling laws developed here represent a superior approach for the collapse of jet spectra. Sample master spectra have been provided in Figs. 3, 4, and 17a–17c, and in [18]. Similar spectra have been generated at all the

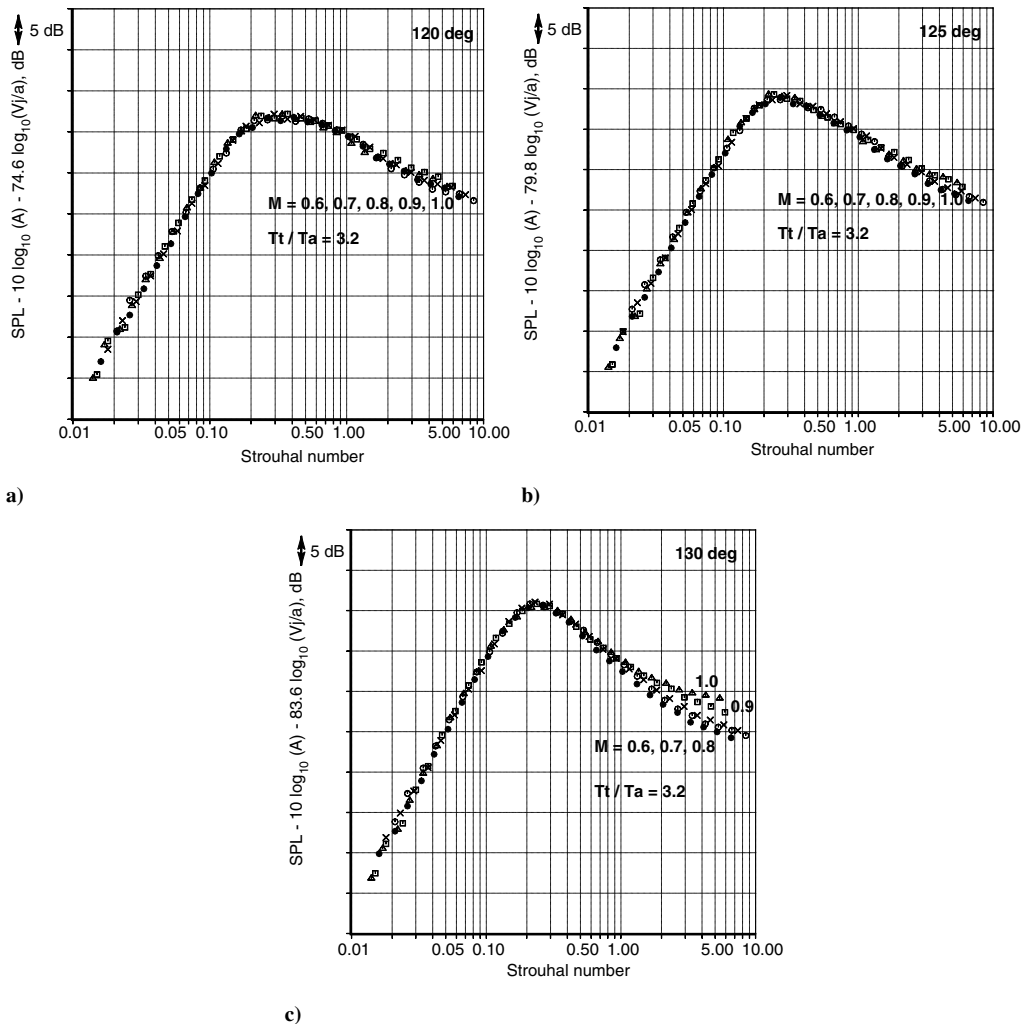


Fig. 17 Normalized spectra from heated jets.

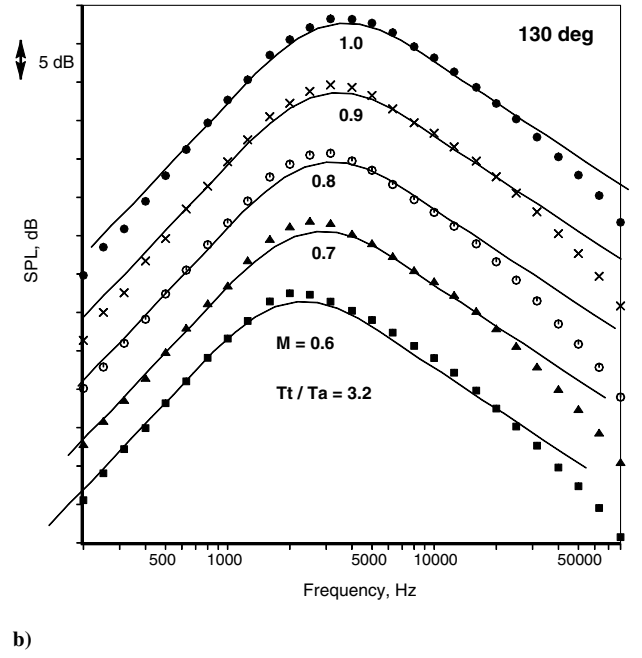
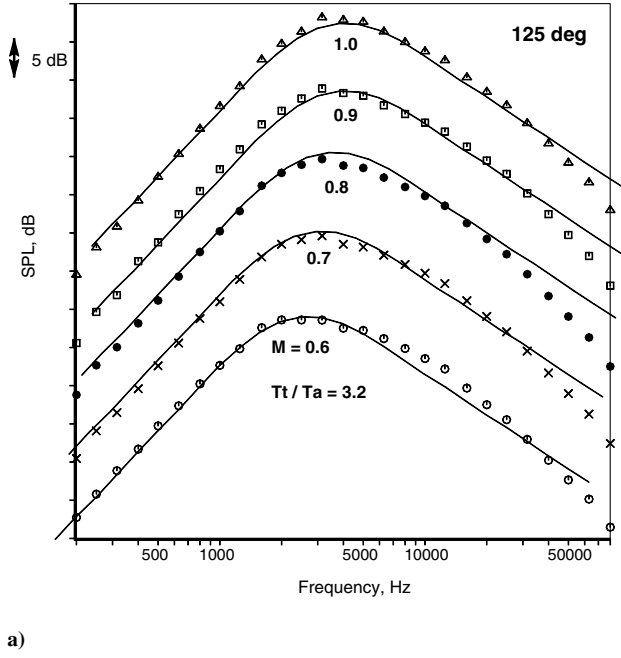


Fig. 18 Comparison of the large-scale similarity (LSS) spectrum with data from heated jets.

angles for all the temperature ratios. As noted, the proper velocity scale must be chosen in the scaling of frequency for angles greater than 130 deg. Before possible approaches are discussed, results from additional analyses that would perhaps shed some light on the angle that demarcates this boundary are presented. The spectral shapes at the two angles of 125 and 130 deg have been examined in detail, and comparisons with the similarity spectra of Tam et al. [21] have been made. Figure 18 compares the measured spectra with the large-scale similarity (LSS) spectra at various Mach numbers of 0.6–1.0. At both the angles, the spectra conform to the LSS shape. An examination of Fig. 14 indicates that the increase in OASPL between these two angles is ~ 1 dB for the lower Mach numbers and ~ 2.5 dB for the higher Mach numbers. Thus, there is no obvious marker, such as a change in spectral shape or a sharp increase in OASPL that can be used to identify the angular range in which nonlinear propagation effects are manifested.

The importance of recognizing the role of the temperature ratio explicitly in the generation of the master spectra is stressed once again with another example; see Sec. V in [18] for more details.

Fig. 19 shows the master spectra at two temperature ratios of 2.2 and 3.2 at an aft angle of 135 deg. Attention is drawn to the fact that the roll off at the higher frequencies is sharper for the jets with higher temperature. The spectral shapes at 90 deg are identical (see Fig. 3 here for example and Fig. 17 in [18]) for all the temperature ratios. An examination of Fig. 2 indicates that for the subsonic jet Mach numbers, the acoustic Mach numbers span a range of 0.43 to 1.36 for $T_t/T_a = 2.2$ and 0.52 to 1.64 for $T_t/T_a = 3.2$. It is obvious that the temperature ratio, rather than the velocity ratio, controls the spectral shape at aft angles. This figure also explains why any directivity factor based solely on (V_j/a) fails to provide the correct spectral shape at the aft angles, thereby disproving the notion that one can predict the spectral shape at the aft angles with a given spectral shape at 90 deg. The above premise is central to the calculation of the effects due to mean flow/acoustic interaction and convective amplification on the sources described by Lilley's equation; see [9,11] for more details on this approach. Based on the results presented here and in [17,18], it is clear that the concept of convective amplification is invalid for jet noise.

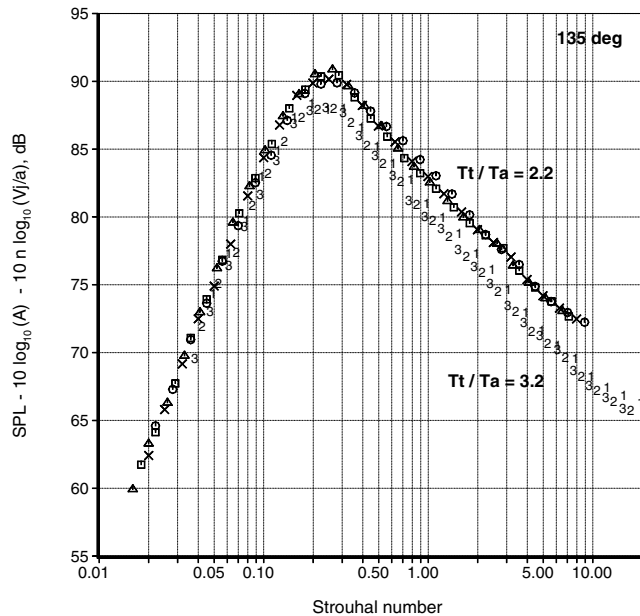


Fig. 19 Normalized spectra from heated jets at various Mach numbers.

V. Maximizing Strouhal Number Range and Making a Prediction

Finally, we demonstrate the versatility of the current approach and the comprehensiveness of the database with a single example. A sample master spectrum is presented at 145 deg for the highest temperature ratio of 3.2 in Fig. 20. For the jets with subsonic convective Mach numbers [jet Mach numbers of 0.7 and 0.8, denoted by \times and \bullet], there is excellent collapse of the data up to a Strouhal number of ~ 17 . Three nozzles of different diameters ($D = 1.5, 2.45$, and 3.46 in.) at three different Mach numbers were used to construct the spectra shown in this figure; therefore, the individual spectra span different ranges of Strouhal numbers. Recall that the raw frequency range is from 200 to 80,000 Hz. With a judicious choice of the jet Mach number and the jet diameter at a particular jet temperature ratio, it is possible to maximize the Strouhal number range of the master spectra. Furthermore, any facility-related tones that tend to occur at fixed raw frequencies can be eliminated with this procedure. This is precisely what is done in Fig. 20. It is noted that the maximum Strouhal number can be further increased to ~ 21 for this (T_t/T_a) . Use of the spectra from the smallest nozzle and at the highest Mach number would extend the range at the lower end. Thus, one can construct the master spectra using all the test points for a given (T_t/T_a) . A crucial point should be kept in mind during this exercise: a

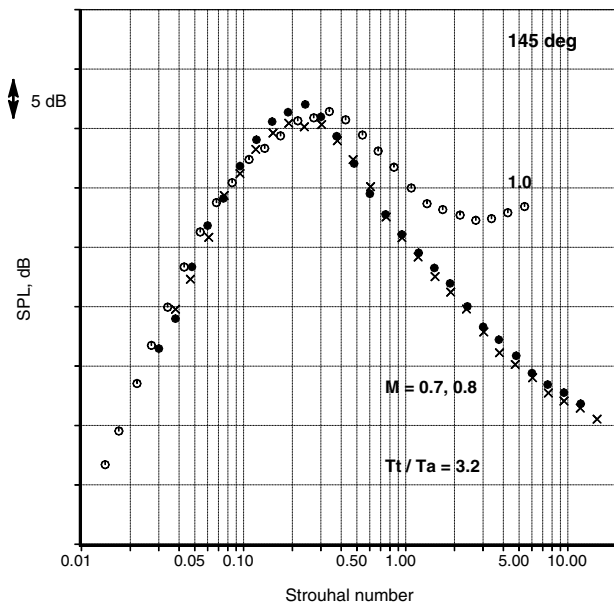


Fig. 20 Master spectrum.

clear understanding of rig noise and its influence on the measured spectra at various test conditions and nozzle diameters is vital to ensure that bad data is not used to generate the master spectra. This point has been emphasized previously by the author; see Viswanathan [14–16].

Figure 20 also indicates the effect of nonlinear propagation at the highest jet Mach number of 1.0. There is no technique available right now to handle this issue. As seen, one could form the master spectra for convectively subsonic jets even in the peak radiation sector, while recognizing the issues already identified here at higher (V_j/a) . As noted, it is quite straightforward to generate the master spectra at the lower angles, outside the peak radiation sector. Further analysis is needed to develop perhaps an “effective velocity” that would align the spectral peak in the angular region of 150 to 160 deg. This is not a new idea; such a strategy has been proposed since the early 1970s and has been incorporated in the SAE method [13]. The steps involved in making a prediction are listed below.

A prediction method entails a simple reversing of the normalization process used to generate the master spectra. The spectral levels can be calculated for any desired jet diameter, Mach number and temperature ratio (jet velocity) through the use of the velocity exponents, at all the desired angles. With the given jet diameter, the spectral levels are adjusted by adding the factor $[10 \times \log_{10}(A)]$ and the Strouhal numbers can be converted to frequency in Hz. The lossless spectra at 20 ft can then be propagated to any desired observer distance with the assumption of linear propagation ($1/r^2$ dependence). Finally, the application of the appropriate atmospheric attenuation corrections (for a desired test day) yields “as-measured” spectra as a function of frequency in Hz. The temperature ratio covers a range of 1.0 to 3.2 and the angular range is from 50 to 155 deg or 160 deg. For any temperature ratio that is not part of the database but within this range, an interpolation is necessary for each angle. For spectra at any intermediate angle, spectral predictions can first be made at the microphone angles of the database and then interpolated. Standard tools and software for multidimensional interpolation from mathematical libraries can be readily used for this purpose.

The Strouhal numbers span a range of 0.01 to ~ 37 for cold jets and 0.01 to ~ 21 for the highest temperature ratio of 3.2. That is, one can make accurate predictions over a very large Strouhal number range without recourse to extrapolation in the frequency space. However, given the smooth variations in the master spectra, it should be possible to extend the range further without incurring too much error. In the SAE [13] method, the frequency parameter $\log_{10}[fD/\xi V_j]$ covers a range of -1.6 to 1.6 . In terms of Strouhal number, this translates to 0.025 to 40. The parameter ξ is empirically determined

and is a function of angle and (V_j/a) ; at the aft angles it reaches a value of ~ 0.5 . The nozzle diameters used to generate the old database on which the SAE method is based are not too dissimilar to the ones used here. However, the high frequency capability of the microphones and the associated electronics used in the early 1970s is restricted to ~ 25 to ~ 32 KHz (at most). Therefore, the maximum measured Strouhal number for the hot jets is perhaps ~ 9 or less. That is, much of the master spectra at the higher Strouhal numbers are extrapolated data and are not real measured data. When the numerous problems with these data due to contamination by extraneous noise sources are factored in, it is clear that the accuracy of the methodology is highly questionable. Other existing empirical prediction methods are also plagued by the same problems. Therefore, it is fair to say that there is no validated and accurate prediction methodology currently available.

VI. Verification of Data Quality

Another, perhaps less obvious, application of the scaling methodology is illustrated with the following examples. Viswanathan [14] demonstrated that it is difficult to acquire good data at low jet velocities with larger nozzles and provided a detailed discussion of the issues that must be addressed in choosing the nozzle size for a particular jet rig and the desired test conditions; see Sec. IV in [14]. With the master spectra, however, it should be possible to make a “prediction” that is superior to the measurements. Figure 21 shows a sample comparison of the predicted spectra (from the master spectra shown in [18]) for an unheated jet at a low Mach number of 0.4 at 90 deg, with the spectra measured with the three different nozzles. The dark symbols and the line represent the prediction and the open symbols the measurements. Clearly, the spectrum from the largest nozzle ($D = 3.46$ in.) is contaminated by rig noise. The smallest nozzle, with $D = 1.5$ in., was first tested and the anomaly at the higher frequencies (denoted by the circles) was noted. Suitable modifications to the jet rig were made to reduce the contamination at the higher frequencies before the nozzle with $D = 2.45$ in. was tested. It is heartening to see the surprisingly good agreement between the prediction and data (denoted by crosses) for the larger nozzle and the efficacy of the rig modifications. A similar comparison at a still lower Mach number of 0.3 is shown in Fig. 22. As at $M = 0.4$, the spectrum from the largest nozzles (triangles) has a higher level of contamination. We also notice that the influence of the rig noise extends to a wider range at the higher frequencies for the smallest nozzle (circles). Again, there is unexpectedly good

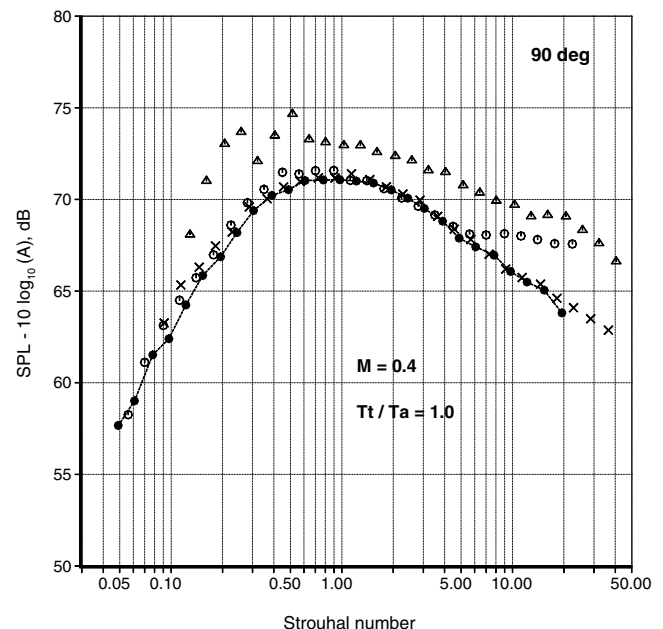


Fig. 21 Comparison of predicted and measured spectra. Solid symbol and line: prediction; \circ : $D = 1.5$ in.; \times : $D = 2.45$ in.; \triangle : $D = 3.46$ in..

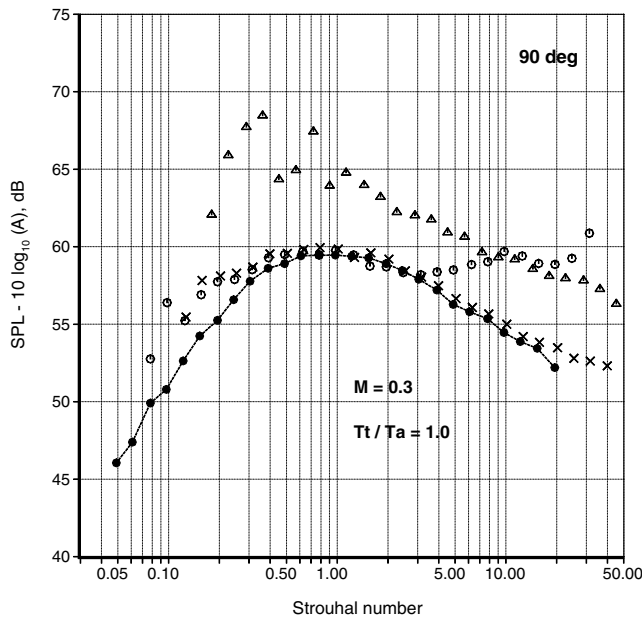


Fig. 22 Comparison of predicted and measured spectra. Solid symbol and line: prediction; \circ : $D = 1.5$ in.; \times : $D = 2.45$ in.; \triangle : $D = 3.46$ in..

agreement for the $D = 2.45$ in. nozzle at the higher frequencies, though there are some blips at the lower frequencies.

The spectra at the very low Mach numbers have not been used in the determination of the velocity exponents. It is gratifying to note the accuracy of the scaling methodology used to generate the master spectra, as evidenced by the prediction of the correct spectral levels and shapes at these lower Mach numbers. Thus, these two figures provide additional validation of the approach adopted here. Furthermore, the master spectra can be used to check the goodness of the measured spectra in a quantitative manner, as demonstrated above.

VII. Conclusions

An accurate empirical prediction method for turbulent mixing noise from single jets has been developed and described. An experimental aeroacoustic database of high quality created by the author and subsequent scaling laws derived using the database have facilitated the development of the prediction method. The scaling laws, wherein the spectral shape at any radiation angle is expressed as a function of the jet velocity ratio and the jet stagnation temperature ratio, allow the spectra at different jet velocities but at a fixed jet temperature to be collapsed to a single curve at each radiation angle. Normalized amplitudes are obtained by removing the effects of the nozzle size (exit area) and the spectral levels are corrected to an arbitrary distance of 20 ft from the center of the nozzle exit plane. Thus, master spectra as a function of the Strouhal number are constructed. The range of the Strouhal number has been extended considerably, when compared with the existing methods, through the use of nozzles of different diameters and the acquisition of accurate data up to a one-third octave centerband frequency of 80 KHz.

It is a trivial matter to obtain excellent collapse of the spectra over the entire frequency range in the angular sector of 50 to 125 deg (from the inlet) using the newly developed scaling laws. In the peak radiation sector, it is straightforward to collapse OASPL, but a deeper analysis is required for scaling the spectra. Several factors need to be considered and the proper velocity scale must be identified. Nonlinear propagation effects are triggered when the convective Mach number becomes supersonic. There is no methodology currently available to account for this phenomenon. The nonlinear effects are confined to radiation angles greater than ~ 130 deg, at least for jet velocities that do not exceed 1850 ft/s (564 m/s). This issue further clouds the spectral scaling in the peak radiation sector. However, it is possible to generate master spectra at all the angles for

jets with subsonic convective Mach numbers. No additional theories or assumptions or empiricisms are needed in the scaling and the generation of the master spectra. As such, a versatile and robust prediction method is a natural outcome of the scaling laws.

A simple reversing of the normalization process used to generate the master spectra leads to a prediction for any desired jet diameter, Mach number and temperature ratio. The master spectra developed here can be used to predict the turbulent mixing noise as well as check the quality of noise data. Further, better quality noise predictions can be made at low jet velocities where accurate measurements are difficult.

References

- [1] Lighthill, M. J., "On Sound Generated Aerodynamically: 1. General Theory," *Proceedings of the Royal Society of London, Series A: Mathematical and Physical Sciences*, Vol. 211, 1952, pp. 564–587.
- [2] Lush, P. A., "Measurements of Subsonic Jet Noise and Comparison with Theory," *Journal of Fluid Mechanics*, Vol. 46, No. 3, 1971, pp. 477–500.
- [3] Hoch, R. G., Duponchel, J. P., Cocking, B. J., and Bryce, W. D., "Studies of the Influence of Density on Jet Noise," *Journal of Sound and Vibration*, Vol. 28, No. 4, 1973, pp. 649–668.
- [4] Fisher, M. J., Lush, P. A., and Harper Bourne, M., "Jet Noise," *Journal of Sound and Vibration*, Vol. 28, No. 3, 1973, pp. 563–585.
- [5] Ahuja, K. K., and Bushell, K. W., "An Experimental Study of Subsonic Jet Noise and Comparison with Theory," *Journal of Sound and Vibration*, Vol. 30, No. 3, 1973, pp. 317–341.
- [6] Morfey, C. L., "Amplification of Aerodynamic Noise by Convected Flow Inhomogeneities," *Journal of Sound and Vibration*, Vol. 31, 1973, pp. 391–397.
- [7] Lilley, G. M., "Aerodynamic Noise," *Noise Mechanisms*, CP-131, AGARD, Brussels, 1974, pp. 13.1–13.12.
- [8] Tanna, H. K., Dean, P. D., and Fisher, M. J., "The Influence of Temperature on Shock-Free Supersonic Jet Noise," *Journal of Sound and Vibration*, Vol. 39, No. 4, 1975, pp. 429–460.
- [9] Tester, B. J., and Morfey, C. L., "Developments in Jet Noise Modelling—Theoretical Predictions and Comparisons with Measure Data," *Journal of Sound and Vibration*, Vol. 46, No. 1, 1976, pp. 79–103.
- [10] Tanna, H. K., "An Experimental Study of Jet Noise. Part 1: Turbulent Mixing Noise," *Journal of Sound and Vibration*, Vol. 50, No. 3, 1977, pp. 405–428.
- [11] Morfey, C. L., Szewczyk, V. M., and Tester, B. J., "New Scaling Laws for Hot and Cold Jet Mixing Noise Based on a Geometric Acoustics Model," *Journal of Sound and Vibration*, Vol. 61, No. 2, 1978, pp. 255–292.
- [12] Lilley, G. M., "Jet Noise Classical Theory and Experiments," in *Aeroacoustics of Flight Vehicles: Theory and Practice, Volume 1: Noise Sources*, edited by H. H. Hubbard, NASA RP-1258, 1995, pp. 211–289.
- [13] Anon, "Gas Turbine Jet Exhaust Noise Prediction," SAE ARP876, Revision D, 1994.
- [14] Viswanathan, K., "Jet Aeroacoustic Testing: Issues and Implications," *AIAA Journal*, Vol. 41, No. 9, 2003, pp. 1674–1689.
- [15] Viswanathan, K., "Aeroacoustics of Hot Jets," *Journal of Fluid Mechanics*, Vol. 516, October 2004, pp. 39–82.
- [16] Viswanathan, K., "Instrumentation Considerations for Accurate Jet Noise Measurements," *AIAA Journal*, Vol. 44, No. 6, June 2006, pp. 1137–1149.
- [17] Viswanathan, K., "Does a Model Scale Nozzle Emit the Same Jet Noise as a Jet Engine?," *AIAA Journal* (to be published).
- [18] Viswanathan, K., "Scaling Laws and a Method for Identifying Components of Jet Noise," *AIAA Journal* (to be published).
- [19] Shields, F. D., and Bass, H. E., "Atmospheric Absorption of High Frequency Noise and Application to Fractional-Octave Band," NASA CR 2760, June 1977.
- [20] Tam, C. K. W., and Tanna, H. K., "Shock Associated Noise of Supersonic Jets from Convergent-Divergent Nozzles," *Journal of Sound and Vibration*, Vol. 81, No. 3, 1982, pp. 337–358.
- [21] Tam, C. K. W., Golebiowski, M., and Seiner, J. M., "On the Two Components of Turbulent Mixing Noise from Supersonic Jets," AIAA Paper 96-1716, 1996.